CONCLUSION

In normal myocardium, BMIPP washout increased with the increase in cardiac work during exercise. In ischemic myocardium, on the other hand, the BMIPP WRs were similar to those in normal myocardium at rest and were not increased by exercise. A certain amount of maximal exercise (net PRP $\geq$ 300×10^3 mmHg/min) was thus found to be necessary to evaluate fatty acid metabolism in normal and ischemic myocardium.

ACKNOWLEDGMENTS

The authors thank Nihon Medi-Physics Co. Ltd. (Nishinomiya, Hyogo, Japan) for its generous donations of BMIPP and to Dr. Hisato Maeda for providing technical assistance.

REFERENCES

1. Knapp FF Jr, Kropp J, Goodman, MM, et al. The development of iodine-123-methyl-branched fatty acids and their applications in nuclear cardiology. *Ann Nucl Med* 1993;7:SII-1–SII-14.
2. Tamaki N, Kawamoto M, Yonekura Y, et al. Regional metabolic abnormality in relation to perfusion and wall motion in patients with myocardial infarction: assessment with emission tomography using an iodinated branched fatty acid analog. *J Nucl Med* 1992;33:659–667.
3. Kropp J, Jorgens M, Glaenzer KP, Luederitz B, Biersack HJ, Knapp FF Jr. Evaluation of ischemia and myocardial viability in patients with coronary artery disease (CAD) with iodine-123-labeled 15-(p-iodophenyl)-3-R,S-methylpentadecanoic acid (BMIPP). *Ann Nucl Med* 1993;7:SII-93–SII-100.
4. Matsunari I, Saga T, Taki J, et al. Kinetics of iodine-123-BMIPP in patients with prior myocardial infarction: assessment with dynamic rest and stress images compared with stress thallium-201 SPECT. *J Nucl Med* 1994;35:1279–1285.
5. Franken PR, DeGeeter FD, Dendale P, Demoor D, Block P, Bossuyt A. Abnormal free fatty acid uptake in subacute myocardial infarction after coronary thrombolysis: correlation with wall motion and inotropic reserve. *J Nucl Med* 1994;35:1758–1765.
6. Nakajima K, Shimizu K, Taki J, et al. Utility of iodine-123-BMIPP in the diagnosis and follow-up of vasospastic angina. *J Nucl Med* 1995;36:1934–1940.
7. Tamaki N, Tadamura E, Kawamoto M, et al. Decreased uptake of iodinated branched fatty acid analog indicates metabolic alterations in ischemic myocardium. *J Nucl Med* 1995;36:1974–1980.
8. Knapp FF Jr, Franken P, Kropp J. Cardiac SPECT with iodine-123-labeled fatty acids: evaluation of myocardial viability with BMIPP. *J Nucl Med* 1995;36:1022–1030.
9. Taki J, Nakajima K, Matsunari I, et al. Impairment of regional fatty acid uptake in relation to wall motion and thallium-201 uptake in ischaemic but viable myocardium: assessment with iodine-123-labelled beta-methyl-branched fatty acid. *Eur J Nucl Med* 1995;22:1385–1392.
10. Franken PR, Dendale P, De Geeter F, Demoor D, Bossuyt A, Block P. Prediction of functional outcome after myocardial infarction using BMIPP and sestamibi scintigraphy. *J Nucl Med* 1996;37:718–722.
11. Kurata C, Tawarahara K, Taguchi T, et al. Myocardial emission computed tomography with iodine-123-labeled beta-methyl-branched fatty acid in patients with hypertrophic cardiomyopathy. *J Nucl Med* 1992;33:6–13.
12. Takeishi Y, Chiba J, Abe S, Tonooka I, Komatani A, Tomoike H. Heterogeneous myocardial distribution of iodine-123 15-(p-iodophenyl)-3-R,S-methylpentadecanoic acid (BMIPP) in patients with hypertrophic cardiomyopathy. *Eur J Nucl Med* 1992;19:775–782.
13. Chen SL, Uehara T, Morozumi T, Yamagami H, Kusuoka H, Nishimura T. Myocardial metabolism of ^{123}I-BMIPP in patients with hypertrophic cardiomyopathy: assessment by radial long-axis SPET. *Nucl Med Commun* 1995;16:336–343.
14. Dudczak R, Schmoliner R, Angelberger P, Knapp FF, Goodman MM. Structurally modified fatty acid: clinical potential as tracers of metabolism. *Eur J Nucl Med* 1986;12:S45–S48.
15. Yamamichi Y, Kusuoka H, Morishita K, et al. Metabolism of iodine-123-BMIPP in perfused rat hearts. *J Nucl Med* 1995;36:1043–1050.
16. Fujibayashi Y, Nohara R, Hosokawa R, et al. Metabolism and kinetics of iodine-123-BMIPP in canine myocardium. *J Nucl Med* 1996;37:757–761.
17. Morishita S, Kusuoka H, Yamamichi Y, Suzuki N, Kurami M, Nishimura T. Kinetics of radioiodinated species in subcellular fractions from rat hearts following administration of iodine-123-labelled 15-(p-iodophenyl)-3-(R,S)-methylpentadecanoic acid (^{123}I-BMIPP). *Eur J Nucl Med* 1996;23:383–389.
18. Ichihara T, Ogawa K, Motomura N, Kubo A, Hashimoto S. Compton scatter compensation using the triple-energy window method for single- and dual-isotope SPECT. *J Nucl Med* 1993;34:2216–2221.
19. Braunwald E, Sobel BE. Coronary blood flow and myocardial ischemia. In: Braunwald E, ed. *Heart disease*, 4th ed. Philadelphia: W.B. Saunders; 1992;1161–1199.
20. Morishita K, Shirakami Y, Kusuoka et al. Uptake and washout kinetics of [I-123]-15-p-iodophenyl-3(R,S)-methyl pentadecanoic acid (BMIPP) in rat hearts [Abstract]. *J Nucl Med* 1996;37:P94–P95.
21. Hosokawa R, Nohara R, Okuda K, et al. Can the metabolism of I-123-BMIPP reflect ischemia? [Abstract]. *J Nucl Med* 1996;37:P95.

Left Ventricular Function and Perfusion in Becker's Muscular Dystrophy

Luigi Mansi, Leonardo Pace, Luisa Politano, Pier Francesco Rambaldi, Fernando Di Gregorio, Pasquale Raia, Vito Rocco Petretta and Giovanni Nigro

Radiology Institute-Nuclear Medicine and Cardiomiology Center; II University of Naples, Naples; Department of Nuclear Medicine, University of Federico II, Naples; and Nuclear Medicine Center of Naples, Italy

The aim of this study was to evaluate left ventricular (LV) perfusion and function in patients with Becker muscular dystrophy (BMD). **Methods:** Fourteen male patients (age range 14–40 yr) with BMD were evaluated by ^{201}Tl SPECT and radionuclide angiography both at rest and after dipyridamole stress test. **Results:** All patients showed uptake defect demonstrated by ^{201}Tl SPECT (mean 4.1 $\pm$ 2.2 uptake defect/patient). Significant relationships ($p < 0.05$) were found between the number of uptake defects and rest LV ejection fraction (LVEF) ($r = -0.54$), peak filling rate (PFR) ($r = -0.57$) and dipyridamole LVEF ($r = -0.65$). Dipyridamole induced reversible uptake defects were found in 7/14 (50%) patients with BMD. The 14 patients were divided into two groups on the basis of the presence (Group A, n = 6) or the absence (Group B, n = 8) of severe irreversible uptake defect (i.e., < 50% ^{201}Tl uptake). Group A showed lower values of PFR and LVEF when compared to patients of Group B. **Conclusion:** In patients with BMD there is a relatively high incidence of uptake defects and LV function (both at rest and after dipyridamole) appears to be related to the number of uptake defects. Moreover, the presence of severe irreversible uptake defects identifies a subgroup of patients with BMD characterized by a severely depressed LV function.

Key Words: thallium-201-SPECT; Becker muscular dystrophy; radionuclide angiography

J Nucl Med 1997; 38:563–567

Becker muscular dystrophy (BMD) is an X-linked recessive muscular disease showing a slowly progressive skeletal muscle disorder with onset in late childhood characterized by weakness of proximal limb girdle muscles and calf muscle hypertrophy (*1–3*). Although muscular symptoms are predominant, heart involvement is a relatively common occurrence with a wide range of cardiac symptoms and manifestations (*4*). Subclinical cardiomyopathy (*5*) as well as dilated cardiomiopathy may be

Received Mar. 12, 1996; accepted Aug. 12, 1996.

For correspondence or reprints contact: Luigi Mansi, MD, Medicina Nucleare-Istituto di Scienze Radiologiche, Seconda Università di Napoli, Piazza Miraglia 2, 80138 Napoli, Italy.

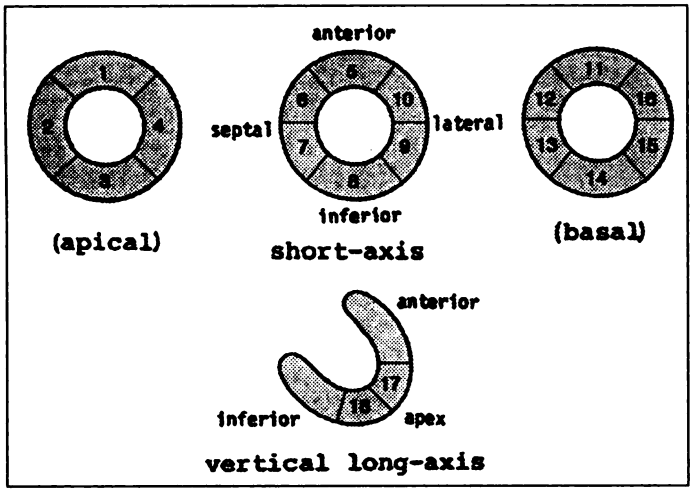

FIGURE 1. Schematic presentation of three short-axis slices and mid-vertical long-axis slice displaying 18 myocardial segments.

present in patient with BMD (*4,6,7*). When cardiac involvement is clinically recognisable, prognosis is usually poor, leading to heart failure, and heart transplantation is often indicated (*8*). Radionuclide evaluation of either function and perfusion of left ventricle may be useful in patient with BMD (*9,10*). The aim of this study was, therefore, to assess cardiac involvement in patients with BMD using radionuclide angiography (RNA) and ^{201}Tl SPECT.

MATERIALS AND METHODS

Study Population

Fourteen consecutive men with BMD (age range 14–40 yr, mean age 28 ± 9 yr) were included in the study. All patients underwent physical examination, blood chemistry work-up, ECG and echocardiogram. Heart involvement was classified, according to Nigro et al. (*4,11*), as preclinical in four patients (shortened PQ segment, prolonged QT interval, increased QT/PQs ratio); arrythmoghenic in four patients (paroxymal tachycardia, WPW syndrome, supraventricular tachycardia, ventricular tachycardia, atrial flutter or fibrillation, BB block, A-V block, sino-atrial block, sick sinus syndrome, sinoatrial dysfunction); dilated cardiomyopathy in six patients (large Q waves in precordial leads, evidence of dilated left ventricle at two-dimensional echocardiography, ejection fraction <45%, PEP/LVET > 0,42). All patients gave informed consent.

Study Protocol

RNA and ^{201}Tl SPECT were performed within 2 wk in all patients. The clinical status did not change in the interval. Both RNA and ^{201}Tl SPECT were performed at rest and after dipyridamole infusion. An intravenous line was installed with a 20 G canula in an antecubital vein. A dose of dipyridamole of 0.56 mg/Kg was diluted in 20 ml of 0.9% saline solution and administered with an infusion rate of 0.140 mg/Kg/min. The duration of the infusion was 4 min. ECG, heart rate and blood pressure were recorded in basal conditions and monitored during dipyridamole infusion. No side effects were observed. All cardiac medications were withdrawn before each radionuclide studies.

Thallium-201 SPECT

SPECT imaging was performed using a single-head, rotating gamma camera with a LEAP collimator. Thallium-201 (74 MBq) was injected 5 min after dipyridamole infusion. Acquisition were performed 5 min and 3 hr after ^{201}Tl administration. Thirty-two projection images were acquired for 40 sec each, with matrix 64 × 64, over a 180° circular orbit from 45° right anterior oblique to 45° left posterior oblique. Energy discrimination was provided by a 20% window positioned on the 80 and 167 keV photopeak of ^{201}Tl. Each study was reconstructed with a Butterworth filter (0.4 cutoff and 5.0 order number). No attenuation correction was performed. Sagittal and oblique tomograms parallel to the long-axis and short-axis of the left ventricle were then extracted from the filtered transaxial tomograms. Myocardial SPECT images were divided into 18 segments for each patient (Fig. 1). These segments were definite as six evenly spaced regions within representative basal and midventricular short-axis tomogram and evenly spaced regions representative of apical short-axis tomogram; moreover, the antero- and infero-apical segments of the mid-vertical long-axis tomogram were included in the analysis (*12*). Two blinded experts interpreted all SPECT images and each segment was scored by consensus using a three point score system (0 = normal ^{201}Tl uptake; 1 = mildly reduced ^{201}Tl uptake; 2 = severely reduced ^{201}Tl uptake). A stress defect, defined as a segment with a ≥1 on dipyridamole

TABLE 1
Patient Data and Radionuclide Angiography and Thallium-201 SPECT Results

Patient no.	Age (yr)	Heart involvement	Radionuclide angiography			^{201}Tl SPECT			
			Rest LVEF (EDV-EDS/EDV %)	Rest PFR (EDV/sec)	Dip LVEF (EDV-EDS/EDV %)	RD	modID	sevID	Total PD
1	17	Preclinical	51%	2.25	60%	1		2	3
2	17	Preclinical	48%	1.90	50%		3		3
3	38	Arrhythmogenic	57%	1.83	61%		2	1	3
4	26	Arrhythmogenic	53%	2.17	64%		3		3
5	37	Arrhythmogenic	61%	1.94	64%		2		2
6	39	Dilated	43%	1.27	45%	2	5	3	10
7	21	Dilated	34%	1.51	27%	4	1	1	6
8	14	Arrhythmogenic	45%	2.23	55%	2			2
9	32	Preclinical	64%	2.97	66%	2	1		3
10	30	Dilated	47%	2.10	52%	7			7
11	18	Preclinical	63%	3.53	75%		3		3
12	34	Dilated	41%	1.29	42%		5		5
13	40	Dilated	19%	0.10	28%		3	2	5
14	25	Dilated	38%	1.66	57%	2		1	3

LVEF = left ventricular ejection fraction; PFR = peak filling rate; RD = reversible defects; modID = moderate irreversible defects; sevID = severe irreversible defects; EDV = end diastolic volume; PD = perfusion defects; Dip = dipyridamole.

TABLE 2
Number and Location of Reversible, Moderate and Severe Irreversible Thallium-201 Defects

Patient no.	Age (yr)	Reversible defects					Moderate irreversible defects					Severe irreversible defects				
		ant	lat	inf	sep	apex	ant	lat	inf	sep	apex	ant	lat	inf	sep	apex
1	17					1								2		
2	17								2		1					
3	38								2							1
4	26								2		1					
5	37								2							
6	39	2						1		2	2		1	2		
7	21	1		1		2			1			1				
8	14				1	1										
9	32			2							1					
10	30	1	1	3		2										
11	18								2		1					
12	34							2	2		1					
13	40							1	1		1		1	1		
14	25			1		1								1		

ant = anterior wall; lat = lateral wall; inf = inferior wall; sep = interventricular septum.

SPECT images, was considered reversible if ^{201}Tl uptake score decreased of at least one point, otherwise it was considered an irreversible defect (ID). Furthermore, ID were subclassified in mild ID (score = 1) and severe ID (score = 2).

Radionuclide Angiography

RNA was performed at rest and during dipyridamole infusion with the patient in the supine position. Red blood cells were labeled in vivo with 740 MBq ^{99m}Tc. Images were acquired with a 1.5x digital zoom in frame mode at a framing rate of 25 msec/frame with a gate tolerance of 5%, collecting at least 150.000 counts/frame using a small field of view gamma camera oriented to a 45° left anterior oblique view with a 15° cranio-caudal tilt.

Left ventricular ejection fraction (LFEV), peak filling rate (PFR), time-to-peak filling rate (TPFR) and peak ejection rate (PER) were computed by a standard computer software.

Statistical Analysis

Data are expressed as proportions or as mean ± one s.d., as appropriate. Spearman rank correlation coefficient (r) was used to assess relationship between a continuous and a polychotomous variable. Differences between proportions were assessed using the chi-square. Differences between mean values were assessed using the Student's t-test. A p value < 0.05 was considered significant.

RESULTS

Table 1 shows the results obtained in the 14 patients with BMD. Dipyridamole LVEF correlated significantly ($r = 0.89$, $p < 0.05$) with rest LVEF. LVEF increased significantly in the whole group (from 47% ± 12% to 53% ± 14%, $p < 0.005$) (Table 1). Table 2 shows the location of Tl defects in the 14 patients studied. All patients showed at least one ^{201}Tl uptake defect. Moderate ID were present in 10/14 (71%) patients, severe ID were observed in 6/14 (43%) patients and reversible defects were present in 7/14 (50%) patients (Table 1). There was a significant relationship between the number of severe ID and PFR ($r = -0.54$, $p < 0.05$). Significant relationships were also found between the total number of Tl uptake defect and rest LVEF ($r = -0.54$, $p < 0.05$), PFR ($r = -0.57$, $p < 0.05$) and dipyridamole LVEF ($r = -0.65$, $p < 0.05$).

The 14 patients were then divided into two groups: Group A with six patients showing at least one severe ID, and Group B with eight patients without severe ID (Table 3). Although an higher number of patients in Group A had dilated left ventricle (67% versus 25%), there were no statistically significant differences in heart involvement between the two groups. On the other hand, either PFR and rest LVEF were significantly ($p < 0.05$) lower in Group A than in Group B (Table 3). Moreover, there was a trend toward lower values of dipyridamole LVEF in Group A, although the difference was not statistically significant.

The 14 patients were finally subgrouped according to their heart involvement (Table 4). Patients with dilatative heart involvement showed a deteriorated left ventricular function and an higher number of ^{201}Tl uptake defects when compared to the other two groups (Table 4). However, a discrete number of ^{201}Tl uptake defect was also found in patients with preclinical heart involvement.

TABLE 3
Relationship Between Patients with Severe Irreversible Thallium-201 Uptake Defects and Patients with Nonsevere Irreversible Thallium-201 Uptake Defects

	Group A (Severe ID) (n = 6)	Group B (Non Severe ID) (n = 8)	p
Patients dilated	4 (67%)	2 (25%)	ns
Patients arrhythmogenic	1 (17%)	3 (38%)	ns
Patients preclinical	1 (17%)	3 (38%)	ns
Age (yr)	30 ± 10	26 ± 9	ns
Rest heart rate (bpm)	73 ± 10	78 ± 9	ns
Rest LVEF (EDV-EDS/EDV%)	40 ± 13	53 ± 9	$p < 0.05$
Rest PER (EDV/sec)	1.7 ± 0.6	2.3 ± 0.5	ns
Rest PFR (EDV/sec)	1.4 ± 0.7	2.3 ± 0.7	$p < 0.05$
Rest TPFR (msec)	164 ± 40	135 ± 38	ns
Dpm heart rate (bpm)	98 ± 8	108 ± 13	ns
Dpm LVEF (EDV-EDS/EDV%)	46 ± 16	59 ± 10	ns
Reversible defects/pts	1.5 ± 1.5	1.4 ± 2.4	ns
ID mod/pts	1.8 ± 1.9	2.1 ± 1.7	ns
Total defects/pts	5.0 ± 2.8	3.5 ± 1.7	ns

LVEF = left ventricular ejection fraction; PFR = peak filling rate; TPFR = time-to-peak filling rate; PER = peak ejection rate; ID = irreversible defects; ID mod = moderate irreversible defects; EDV = end diastolic volume; ESV = end systolic volume; Dpm = dipyridamole.

TABLE 4
Correlation Between Patients with Preclinical, Arrhythmogenic and Dilated Heart Involvement

	Preclinical	Arrhythmogenic	Dilated
Age (yr)	21 ± 7	29 ± 11	32 ± 8
Rest heart rate (bpm)	78 ± 11	77 ± 9	72 ± 10
Rest LVED (EDV-ESV/EDV%)	57 ± 8*	54 ± 7*	37 ± 10
Rest PER (EDV/sec)	2.4 ± 0.6	2.3 ± 0.3	1.5 ±t0.3
Rest PFR (EDV/sec)	2.7 ± 0.7*	2.0 ± 0.2	1.3 ± 0.7
Rest TPFR (msec)	133 ± 28	142 ± 56	163 ± 40
Dpm heart rate (bpm)	106 ± 14	103 ± 10	103 ± 15
Dpm LVEF (EDV-ESV/EDV%)	63 ± 11*	61 ± 4*	42T± 12
RD/pt	0.8 ± 1.0	0.5 ± 1.0	2.5 ± 2.7
ID mod/pt	1.8 ± 1.5	1.8 ± 1.3	2.3 ± 2.3
ID sev/pt	0.5 ± 1.0	0.3 ± 0.5	1.2 ± 1.2
Total defects/pt	3.0 ± 0.6*	2.5 ± 0.6*	6.0 ± 2.4

* = $p < 0.05$ vs dilated.

LVEF = left ventricular ejection fraction; PFR = peak filling rate; TPFR = time-to-peak filling rate; PER = peak ejection rate; EDV = end diastolic volume; ESV = end systolic volume; RD = reversible defect; ID mod = moderate irreversible defect; ID sev = severe irreversible defect; Dpm = dipyridamole.

DISCUSSION

This study reports the findings in 14 patients with BMD studied with RNA and ^{201}Tl SPECT at rest and after dipyridamole infusion. All patients showed ^{201}Tl uptake defects, and 50% of them had dipyridamole-induced uptake defect. The total number of ^{201}Tl uptake defect per patient was significantly correlated with either diastolic and systolic (both at rest and during dipyridamole infusion) left ventricular function. This finding seems to confirm previous observations suggesting that cardiac dysfunction is a primary feature in BMD (*4,13*). Recent studies have demonstrated in cardiac biopsy specimen the same dystrophic lesion as in skeletal muscle (*14–16*), suggesting that heart involvement in BMD patients may be due to the expression of an altered dystrophin and not be secondary to the skeletal muscle disease. Moreover, it has been demonstrated that BMD cardiomyopathy evolves unrelated to musculoskeletal involvement, and is the primary cause of death among these patients (*4,5*).

The results of this study suggest that left ventricular dysfunction is related not only to the number of ^{201}Tl uptake defects but also to their severity. In fact, when the patients were grouped according to the presence or not of severe ID (Table 3), those with severe ID had lower values of rest LVEF and PFR. Since the presence of severe ID can be related to myocites necrosis, which is the final step of the pathological process of myocardial involvement in BMD, it is not surprising to find more impairment in LV function in patients showing severe ID.

In the group of patients included in this study, 4 (29%) were classified as having preclinical heart involvement, and all had ^{201}Tl defects, although showing a lower extent of myocardial abnormalities than patients with dilated left ventricle. In addition, patients with preclinical heart involvement had preserved LV systolic and diastolic function. Since it has been suggested that preclinical cardiomyopathy tends to evolve to clinically evident cardiac disease (*4*), it is conceivable that ^{201}Tl SPECT could be used to identify BMD patients with early heart involvement, and thus to better define therapeutic strategies in these subjects.

A total of 58 defects were found in the 14 patients (mean 4 ± 2). Of these 58 ^{201}Tl defects, 10 (17%) in six patients (mean 1.7 ± 0.8) were classified as severe ID. These severe ID were considered expression of fibrous tissue replacement. However, since no reinjection or late redistribution were performed, we cannot exclude that some of these severe ID could have shown enhanced ^{201}Tl uptake.

Dipyridamole induced LV abnormalities in patients with BMD have been previously reported (*17*). In this study, rest and dipyridamole RNA was performed in order to confirm these data. Dipyridamole stress test is a well known alternative to exercise stress test in patients who cannot perform it, such as BMD patients. It is safe and highly specific in various cardiac diseases (*18–20*). In the 14 BMD studied, LVEF increased significantly after dipyridamole.

In this study we found the presence of ^{201}Tl uptake reversible defect in 50% of the patients with BMD. In particular, 20 reversible defects were observed in seven patients (2.8 ± 2). This feature is partially unexpected in those subjects where myocardial involvement should be mainly due to replacement of myocites by fibrous tissue. These results can be suggestive of a different pathological process, affecting to some extent myocardial perfusion. Moreover, recently an increased number of mast cells have been shown to accumulate in degenerating muscle tissue and to secrete vasoconstrictor cytokines, thus potentiating muscle damage through an ischemic mechanism (*21*) in addition to the well known altered membrane permeability and replacement of myocites by fibrous tissue (*10*).

Since none of the patients included in this study underwent coronary angiography, the presence of coronary artery stenoses cannot be excluded. However, previous studies demonstrated the absence of luminal narrowing of either extramural or intramural coronary arteries in patients with muscular dystrophy (*22,23*).

The results of this study suggest the presence of myocardial abnormalities in BMD patients even in the absence of clinically evident heart involvement. Although these finding are based on a relatively small population, the data indicate a potential role of radionuclide imaging in the early detection of cardiac involvement in BMD patients.

ACKNOWLEDGMENTS

We thank Professor Paola Tesauro for her invaluable contribution in this study. This work was supported by a grant of Italian Telethon to the Institute of Radiological Sciences-Nuclear Medicine, II University of Naples, Italy (principal investigator Professor Paola Tesauro).

REFERENCES

1. Emery AEH, Dreifuss FE. Unusual type of benign X-linked muscular dystrophy. *J Neurol Neurosurg Psychiatry* 1966;29:338–342.
2. Markand ON, North RR, D'Agostino AN, Dali DD. Benign sex-linked recessive muscular dystrophy. *Neurology* 1969;19:617–633.
3. Ringel SP, Carrol JE, Schold SC. The spectrum of mild X-linked recessive muscular dystrophy. *Arch Neurol* 1977;34:408–416.
4. Nigro G, Comi LI, Politano L, et al. Evaluation of the cardiomyopathy in Becker muscular dystrophy. *Muscle Nerve* 1995;18:283–291.
5. de Visser M, de Voogt WG, la Rivière GV. The heart in Becker muscular dystrophy, fascioscapulohumeral dystrophy and Bethlem myopathy. *Muscle Nerve* 1992;15:591–596.
6. Lazzaroni E, Favaro L, Botti G. Dilated cardiomyopathy with regional myocardial hypoperfusion in Becker's muscular dystrophy. *Int J Cardiol* 1989;22:126–129.
7. Sakata C, Yamada H, Sunohara N, Arahata K, Nonaka I. Cardiomyopathy in Becker muscular dystrophy. *Rinsho Shinkeigaku* 1990;30:952–955.
8. Orlov YSK, Brodsky MA, Allen BJ, Ott RA, Orlov MV, Jay CA. Cardiac manifestation and their management in Becker's muscular dystrophy. *Am Heart J* 1994;128: 193–196.
9. Steare SE, Dubowitz V, Benatar A. Subclinical cardiomyopathy in Becker muscular dystrophy. *Br Heart J* 1992;68:304–308.
10. Yamamoto S, Matsushima H, Suzuki A. A comparative study of thallium-201 SPECT and electrocardiography in duchenne and in other types of muscular dystrophy. *Am J Cardiol* 1988;61:836–43.
11. Nigro G, Comi LI, Politano L, Bain RJI. The incidence and evolution of cardiomyopathy in Duchenne muscular dystrophy. *Int J of Cardiol* 1990;26:271–277.
12. Kiat H, Germano G, Friedman J, et al. Comparative feasibility of separate or

simultaneous rest thallium-201/stress technetium-99m-sestamibi dual-isotope myocardial SPECT. *J Nucl Med* 1994;35:542–548.
13. Goldberg SJ, Feldman L, Reinecke C, Stern LZ, Sahn DJ, Hallen HD. Echocardiographic determination of contraction and relaxation measurements of the left ventricular wall in normal subjects and in patients with muscular dystrophy. *Circulation* 1980;62:1061–1069.
14. Sanyal SK, Jonson WW, Thapar MK, Pitner SE. An ultrastructural basis for electrocardiographic alterations associated with Duchenne's muscular dystrophy. *Circulation* 1978;57:1122–1148.
15. Frankel KA, Rosser RJ. The pathology of the heart in progressive muscular dystrophy: epimyocardial fibrosis. *Hum Pathol* 1976;7:375–386.
16. Melacini P, Fanin M, Danieli GA, et al. Cardiac involvement in Becker muscular dystrophy. *J Am Coll Cardiol* 1993;22:1927–1934.
17. Comi LI, Politano L, Limongelli FM, et al. Cardiological and enzymatic changes following stress test in Becker patients. *Acta Cardiomiologica* 1990;1:67–73.
18. Cates CU, Kronenberg MW, Collins HW, Sandler MP. Dipyridamole radionuclide ventriculography: a test with high specificity for severe coronary artery disease. *J Am Coll Cardiol* 1989;13:841–851.
19. Picano E, Lattanzi F, Masini M, Distante A, L'Abbate A. Usefulness of dipyridamole-echocardiography test for diagnosis of syndrome X. *Am J Cardiol* 1987;60:508–512.
20. Lazzeroni E, Picano E, Dodi C, et al. Dipyridamole echocardiography for diagnosis of coexistent coronary artery disease in hypertrophic cardiomyopathy. *Am J Cardiol* 1995;75:810–813.
21. Gorospe JR, Thorpe MD, Hinckley J, Kornegay JM, Hofmann EP. A role for mast cells in the progression of the Duchenne muscular dystrophy? Correlation in dystrophin—deficient humans, dog and mice. *J Neurolog Sci* 1994;122:44–56.
22. Skyring A, McKusick VA. Clinical, genetic and electrocardiographic studies in childhood muscular dystrophy. *Am J Med Sci* 1961;242:534–547.
23. Perloff JK, Henze E, Schelbert HR. Alterations in regional myocardial metabolism, perfusion and wall motion in Duchenne muscular dystrophy by radionuclide imaging. *Circulation* 1984;1:33–42.

Assessment of Cardiac Sympathetic Function with Iodine-123-MIBG Imaging in Obstructive Sleep Apnea Syndrome

Naoki Otsuka, Motoharu Ohi, Kazuo Chin, Hideo Kita, Tetsuo Noguchi, Tatsuhiko Hata, Ryuji Nohara, Ryohei Hosokawa, Masatoshi Fujita and Kenshi Kuno

Department of Clinical Physiology, Chest Disease Research Institute, and the Third Department of Internal Medicine, Kyoto University, Kyoto, Japan

Iodine-123-MIBG imaging has been used to evaluate myocardial sympathetic function in various cardiac diseases. In patients with obstructive sleep apnea syndrome (OSAS), increased sympathetic activity has been widely recognized, as assessed by measuring the plasma concentration and urinary excretion of catecholamines and by measuring muscle sympathetic nerve activity. However, these measurements are not specific indices of cardiac sympathetic function. Therefore, this study was undertaken to assess cardiac sympathetic function in patients with OSAS using MIBG cardiac scintigraphy. **Methods:** This study consisted of 11 patients (10 men, 1 woman; mean age 43 ± 16 yr) with a diagnosis of OSAS established by polysomnography, and 8 age-matched normal control subjects (7 men, 1 woman; mean age 45 ± 18 yr). Early (15 min) and delayed (3 hr) planar images were taken after the injection of 111 MBq of [^{123}I]MIBG. The mean counts of the whole heart and the mediastinum were obtained to calculate heart-to-mediastinum count ratios from the early images (H/Me) and from the delayed images (H/Md) and the myocardial washout rate (WR). Eight patients were restudied after 1 mo of nasal continuous positive airway pressure treatment. **Results:** The H/Me and H/Md ratios were significantly lower in the patients than in the control subjects (H/Me, 2.49 ± 0.32 versus 2.84 ± 0.34, p = 0.0207; and H/Md, 2.33 ± 0.30 versus 3.02 ± 0.36, p = 0.0013). The WR was higher in the patients than in the control subjects (36.2 ± 9.0% versus 23.6 ± 4.9%, p = 0.0022). The H/Me and H/Md ratios in the patients were significantly correlated with the apnea-hypopnea index and the degree of hypoxemia during sleep. After treatment, H/Me and H/Md remained unchanged, but WR significantly recovered (from 34.9 ± 10.4% to 26.3 ± 7.7%, p = 0.0357). **Conclusion:** Cardiac sympathetic function and integrity are impaired in subjects with OSAS when compared with age-matched control subjects. MIBG cardiac imaging can be helpful in evaluating cardiac involvement and efficacy of therapy in OSAS.

Received Apr. 1, 1996; revision accepted Aug. 12, 1996.

For correspondence or reprints contact: Naoki Otsuka, MD, Department of Clinical Physiology, Chest Disease Research Institute, Kyoto University, Shogoin-Kawaharacho 53, Sakyo-ku, Kyoto 606-01, Japan.

Key Words: obstructive sleep apnea syndrome; iodine-123-MIBG; cardiac sympathetic function

J Nucl Med 1997; 38:567–572

Obstructive sleep apnea syndrome (OSAS) is a condition characterized by repetitive cycles of upper airway occlusion, resulting in repeated inspiratory efforts against this occlusion. Reopening of the upper airway usually follows an arousal from sleep. The resumption of airflow is characterized by a brief period of hyperventilation with snoring, and a subsequent return to sleep. Several hemodynamic changes occur during this apnea/ventilation cycle (*1*). OSAS has been associated with long-term cardiovascular sequelae, including systemic and pulmonary hypertension, heart failure, arrhythmias, stroke and myocardial infarction (*2,3*). In addition, there appears to be an excess of cardiovascular mortality in untreated OSAS (*4–6*). The exact causes of this increased cardiovascular morbidity are unknown. However, in patients with OSAS, increased sympathetic activity has been reported during sleep with repetitive apnea and even while the patients were awake (*7–12*). Increased sympathetic activity has been thought to contribute significantly to the pathophysiology of myocardial infarction, arrhythmia, heart failure and sudden death (*13,14*). Taken together, this sympathetic activation may be one of the causative factors of the increased mortality and the frequent cardiovascular complications mentioned above. Sympathetic function in OSAS has been assessed by measuring plasma concentration (*7,8*) and urinary excretion (*9,10*) of catecholamines, and by measuring muscle sympathetic nerve activity (MSNA) (*11,12*). However, these parameters are not specific indices of cardiac sympathetic activity.

Metaiodobenzylguanidine (MIBG), an analog of guanetidine, shares many neuronal transport and storage mechanisms with norepinephrine (NE) (*15–17*). Noninvasive radionuclide imaging with [^{123}I]MIBG permits assessment of efferent adrenergic